Mechanical and Interfacial Properties Characterisation of Single Carbon Fibres for Composite Applications

**X. Ji · C. Wang · B.A.P. Francis · E.S.M. Chia · L. Zheng ·
J. Yang · S.C. Joshi · Z. Chen**

Abstract The mechanical and interfacial properties of single carbon fibres have been experimentally investigated. Longitudinal tensile strengths were determined using single filament as well as impregnated yarn specimens at various gauge lengths ranging from 5 to 200 mm. The tensile behaviour of the fibre depends on gauge length due to the presence of flaws along the fibre. Axial compressive strength was obtained by the tensile recoil method. The transverse modulus was measured by nano-indentation technique. Shear modulus was obtained by a torsional pendulum test. The apparent shear strength of carbon fibre/epoxy interface was characterised by a microbond fibre pull-out test. Data obtained in this work constitute important materials' data input for the design and simulation of carbon fibre composite structures.

X. Ji · B.A.P. Francis · S.C. Joshi · Z. Chen
Temasek Laboratories@NTU, 50 Nanyang Drive,
Singapore 637553, Singapore

C. Wang · Z. Chen (✉)
School of Materials Science and Engineering, Nanyang
Technological University, Singapore 639798, Singapore
e-mail: aszchen@ntu.edu.sg

E.S.M. Chia
DSO National Laboratories, 20 Science Park Drive,
Singapore 118230, Singapore

L. Zheng · J. Yang · S.C. Joshi
School of Mechanical and Aerospace Engineering, Nanyang
Technological University, Singapore 639798, Singapore

Introduction

Since the inaugural commercial appearance in 1879 [1], carbon fibres and textile preforms have been extensively used as reinforcements in polymer based composites. Over the past decades, researchers and engineers have increasingly utilised a variety of analytical and numerical methods including micromechanical modelling and finite element analysis (FEA) to predict the homogenised properties of composites and their damage behaviours (see for example [2–6]). The accuracy of such analysis is subject to not only an appropriate definition of the model but also the credibility of materials property inputs. As the principle load-carrying constituent in many advanced applications, carbon fibre and its mechanical properties warrant special scrutiny.

There have been research efforts in understanding the mechanical behaviours of various high-performance fibres [7–12]. However, documented experimental results on carbon fibres are still limited and incomprehensive. A majority of literature focused either on one aspect of carbon fibre properties [13–15] or on certain experimental technique [16, 17]; while few published works attempted to comprehensively characterise the mechanical and the interfacial properties of one type of carbon fibre. It remains a great challenge to characterise fibre materials because there are no widely-accepted standards for specific test of fibre properties despite many methodologies have been proposed. In addition, the extremely high disparity between published properties of carbon fibre [18–22] confuses users further should they look into literature for input data for their distinctive numerical simulations, analytical calculations and engineering composites design. In this study, mechanical and interfacial properties of a type of commercially available carbon fibres produced by an international manufacturer have been measured experimentally. The study is designed to fill the gap, improve the accuracy of the test methods and then apply them to a new type of carbon fibre.

The results in this paper can serve as reliable references for further investigation of the carbon fibre or as inputs in multi-scale simulation of fibrous composites.

Experimental and Results

Material

The tested fibre is the PAN (Polyacrylonitrile)-based AKSAca A-42 carbon fibre with bulk density of 1.78 g/cm^3 and yield of 800 g/km, respectively. A high-resolution Field Emission Scanning Electron Microscope (FE-SEM) image of a single fibre is shown in Fig. 1. The fibre diameter was determined to be 7.3±0.4 μm.

Longitudinal Tensile Test

In this study, due to the specimen size restriction of the home-designed micro-tester, short-gauge-length single filaments were tested in accordance to ASTM Standard C1557-03 (see Fig. 2). The single filament specimen was prepared by mounting a single carbon fibre to a paper holder with instant cyano-acrylate glue. The sample was placed in the grips of the micro-tester equipped with a 250 g-force (gf) load cell. Both sides of the paper holder were cut by scissors before testing, leaving the fibre between the grips intact. Single filament specimens with gauge lengths of 5, 10, 15 and 20 mm were tested at the speed of 0.001 mm/s. A minimum of 10 specimens were tested for each gauge length. To test large-gauge-length resin-impregnated fibre yarns, an Instron universal tester was employed following ISO standard 10618:2004. A yarn with 12,000 fibres was impregnated with 40 % weight ratio of Bakelite L20 epoxy resin and cured for 24 h at room temperature followed by 15 h of heat treatment at 60 °C before aluminium tabs were mounted at its two ends. Samples with gauge lengths of 50, 100, 150 and 200 mm were tested at the speed of 2 mm/min.
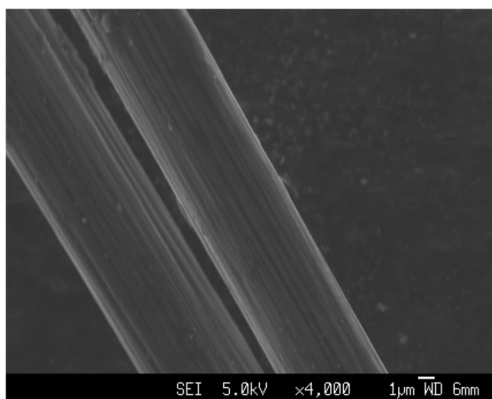

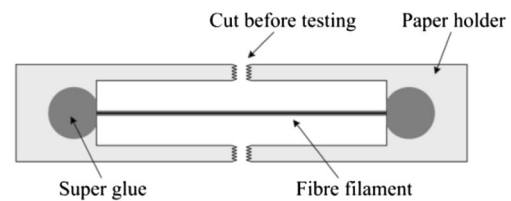**Fig. 1** FE-SEM image of a single carbon fibre

Fig. 2 Single filament specimen with cut paper holder

It should be noted that as the strain measurement of the tests was done by measuring the movement of the grip of the single fibre tester, system compliance correction had to be performed according to the procedure described in ASTM C1577-03. In the study, the system compliance (C_s) was determined by plotting $\Delta L/F$ (C_a, apparent compliance) against l_0/A curve in which ΔL is the grip movement measured from the machine, F is the failure load, A is the cross-sectional area of carbon fibre and l_0 is the gauge length of the sample. In Fig. 3, the intercept corresponds to zero gauge length gives the value of C_s, which is 0.022 mm/N. The compliance of the tensile test system influences the calculated strain and Young's modulus, especially when the sample gauge length is small. The results presented in this study have been calibrated for the compliance.

As shown in Fig. 4, the tensile behaviour of the carbon fibre, in both dry single filament and impregnated yarn form, is linear elastic till brittle fracture occurs. Moreover, the tensile strength of the carbon fibre is a complex parameter which is inappropriate to describe with a single value [23, 24]. The gauge length effect is a reflection of the distribution of flaws along the fibre. There are several theories that describe the gauge length effect of tensile strength like 'chain of links' model [25]. Basically, for brittle fibre materials, the strength is determined by the weakest point along the tested length. Therefore, the longer the gauge length, the higher the chance of finding a more severe flaw
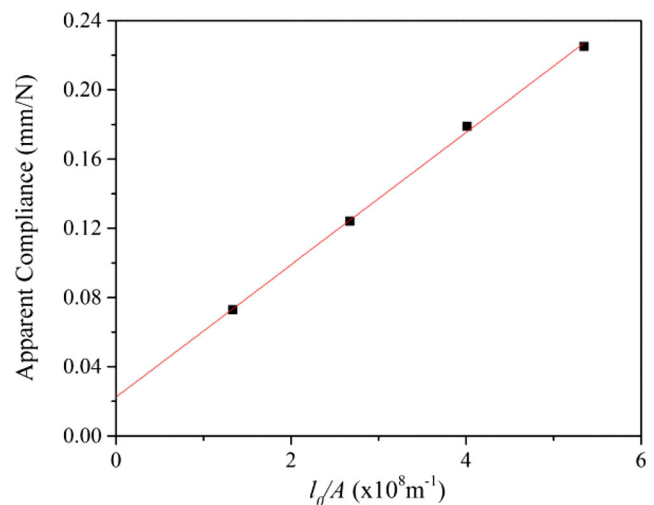

Fig. 3 Apparent compliance versus gauge length divided by cross-sectional area of carbon fibre
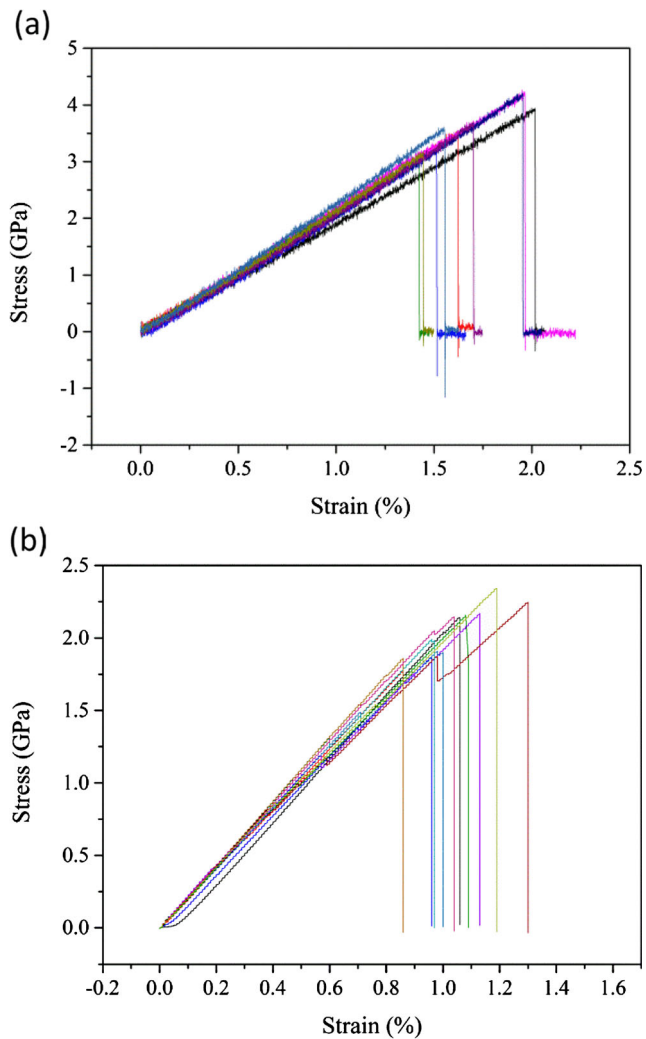
(a)

(b)

Fig. 4 Tensile stress-strain curves for (**a**) single filament samples at gauge length 10 mm and (**b**) impregnated yarn samples at gauge length 200 mm

Fig. 5 Tensile strength of the carbon fibre as a function of gauge length. Inset is the plot when the gauge length is presented in a log scale

In addition, gauge length effect is also observed in calculating longitudinal Young's modulus (E_1). The average value of E_1 for gauge lengths of 5, 10, 15 and 20 mm were determined to be 191.8, 224.0, 227.2 and 239. 5 GPa, respectively. The gauge length effect of on E_1 can be attributed to the initially mis-oriented crystallites of carbon fibre which control the value of the elastic modulus [26]. When the fibre length is small, the effect of the mis-oriented sections of fibre crystallites is more prominent. In contrast, as the fibre length increases, there is more uniformity along the axis on average and the initial stretching and fibre misalignment relatively reduces [27].

Longitudinal Compressive Strength by Tensile Recoil Method

The longitudinal compressive properties of carbon fibre is technically more challenging to obtain than its tensile counterparts, primarily due to the difficulty in introducing a pure axial compressive failure to a carbon fibre without causing buckling [28]. Among the methods proposed [29–31], tensile recoil method [32] is preferred by many [33, 34] thanks to its procedural simplicity and reliability to produce repeatable results.

In the tensile recoil method, a single fibre is stretched to a predetermined tensile stress level to allow some strain energy to be stored in the fibre. Then the fibre is cut by a sharp surgical scissor in the middle of the gauge length, initiating a recoil effect. When the fibre is cut, the tensile stress in the fibre drops to zero, converting the stored strain energy to kinetic energy. A kinetic energy wave thus propagates towards the clamped ends. The moment the stress wave reaches the rigid end, the strain energy is completely converted to kinetic energy. Hitting the rigid end, the kinetic energy will be converted back to strain energy. During this snap-back process, a compressive

which leads to a lower strength. The fibre flaws may include micropores, fibril misalignments and impurities, and are usually generated during processing and handling. The presence of fibre flaws may be either on the surface or inside the bulk (volume flaws). As shown in Fig. 1, the surface grooves are clearly visible, but we are not able to detect the internal (volume) flaws due to its small sizes. Nevertheless, it is reasonable to argue that for fibres of a few microns in diameter, surface flaw is probably much more important in determining its strength. In general, the presence of flaws at random locations not only leads to scatter in the experimentally determined values of strength for a fixed length of fibre but also to a decreasing strength as gauge length increases. Hence, the strength of carbon fibre is better reported as gauge length dependent values. The effect of gauge length is especially prominent when gauge length is small (see Fig. 5). The observed trend agrees well with the results obtained by others [25].
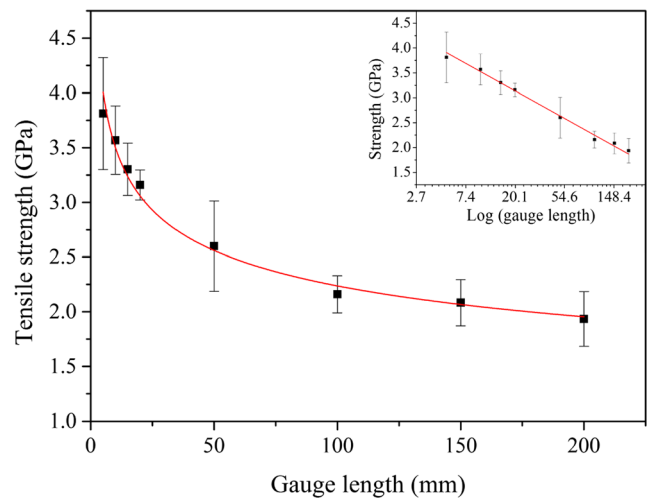
stress which equals to the pre-applied stress in magnitude is generated. If the resultant compressive stress exceeds the compressive limit of the fibre, the fibre undergoes recoil compressive damage (see Fig. 6). As such, by increasing the pre-stress level in a precise manner from a magnitude that is below the compressive strength of the fibre to a magnitude that exceeds the compressive strength, a transition in the damage behaviour of carbon fibre from no recoil compressive damage to some recoil compressive damage will be observed. Hence a threshold stress for observation of recoil compressive damage can be established to approximate the compressive strength of carbon fibre.

The samples were tested by a dedicated tensile machine, apt-dc servo controller Thorlabs Z812B, with a load cell of 20 gf. The pieces of the filament after testing were carefully examined under a magnifying glass to determine if they had failed (F) or not (NF). A total of 400 fibre samples, split into 8 batches, were tested. The results of the recoil compressive failure test were analysed by two methods [33]. In the first method, the predetermined stress levels for each batch were arranged in an ascending order. Two stress levels under which the fibre exhibited the last complete survival (NF, NF) and the first complete failure (F, F) on both ends were identified. Thereby, a threshold value was calculated by averaging the two stress levels. Table 1 tabulates the experimental data for one of the eight batches. Each table entry is one test sample from which two observations (top end and bottom end) were obtained. Two stress levels of 693.5 and 758.7 MPa were identified to be corresponding to 100 % survival and 100 % failure; therefore, the magnitude of compressive strength for this batch of specimen was determined to be 726.1 MPa for this batch. In this method the recoil compressive strength is identified by the maximum stress of 100 % survival and the minimum stress 100 % failure. Therefore, more test samples and more precise control of pre-stress are needed to reduce the stress range.
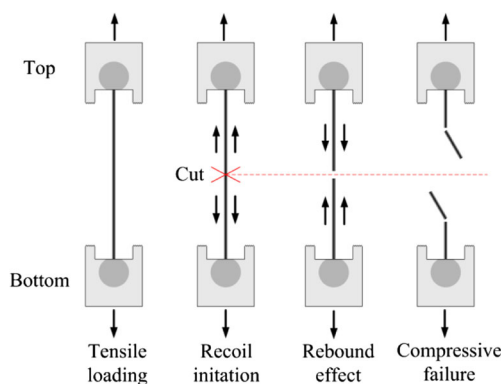
Table 1 Ranked recoil failure data for one batch (NF – not failed, F – failed)

Pre-stress (MPa)	Top end	Bottom end
631.4	NF	NF
656.4	NF	NF
665.2	NF	NF
690.1	NF	NF
693.5	*NF*	*NF*
725.0	NF	F
758.7	*F*	*F*
767.8	F	NF
773.3	F	F
783.7	F	F
791.2	F	F

In the second method which is based on probabilistic model developed by Jiang et al. [34], a logistic distribution was fitted for the entire 400 samples to determine the compressive strength of the carbon fibre. It is assumed that the recoil failure at either end is an independent process. Therefore this process is assumed to be governed by the same probability distribution. The probability of failure $F(\sigma)$ was plotted against the midpoint of corresponding recoil stress range. Figure 7 shows the fitted logistic distribution curve. The mid recoil stress corresponds to the probability of failure of 0.5, when the fibre has equal probability of failure and survival, signifies the compressive strength. The fitted curve in Fig. 7 gives the compressive strength value of 721.2 MPa. It is claimed that this method shows much less variation and is well suited even when a wide stress range data are involved in the test because the fitted curve provides better accuracy [33]. The compressive strength values obtained by the aforementioned two methods are summarised in Table 2. The two results are similar in an acceptable range indicating that both methods are able to get
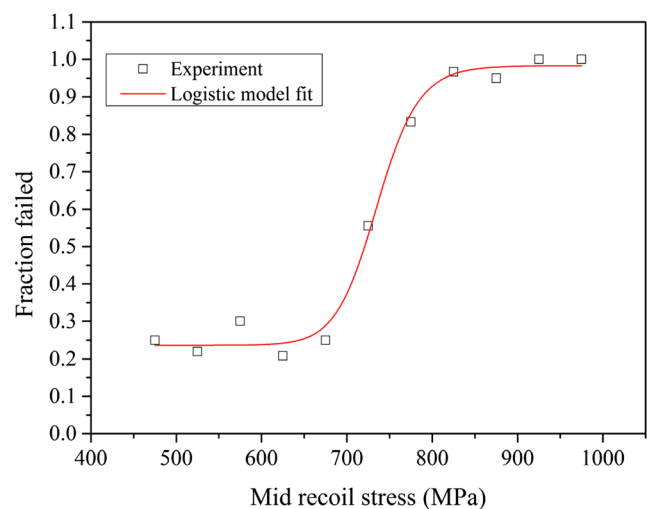

Fig. 6 Illustration of the tensile compressive failure process

Fig. 7 Probability of failure versus mid recoil stress with Logistic model fit

**Table 2** Summary of the compressive strength results in MPa

Method 1				Method 2
Batch 1	715.4	Batch 5	713.4	721.2
Batch 2	842.2	Batch 6	736.3	
Batch 3	667.9	Batch 7	726.1	
Batch 4	740.6	Batch 8	749.7	
Mean				736.4
Mean strength of the two methods				728.8

reasonable results when the test data were quantitatively sufficient. Therefore, we reported an average value of those two methods at 728.8 MPa.

Longitudinal Shear Modulus by Torsional Pendulum Test

The longitudinal shear modulus of the carbon fibre was determined by torsional pendulum tests. The theoretical background is that a disk hung by a wire will oscillate about its equilibrium position if it is twisted by a small angle. Although the magnitude of the oscillation will decrease, the frequency of oscillation is a function of the longitudinal shear modulus of the wire.

In this study, a washer, suspended by a single carbon fibre, was set in free torsional oscillation without air turbulence (Fig. 8). The fibre was attached on the washer using cyanoacrylate glue. The washer was twisted by slight touch using the tip of a tweezer. To make sure that the fibre was aligned in the
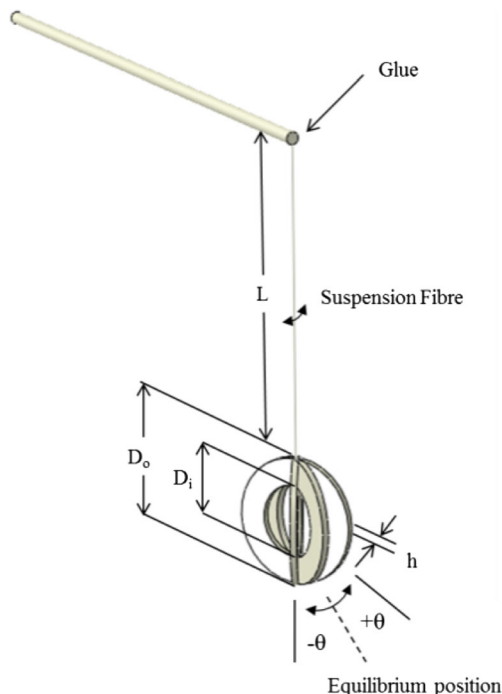
Fig. 8 The experiment setup of torsional pendulum test

centre of mass of the washer, the perpendicular bisector was marked first on the washer and the fibre was attached carefully according the marked position.

The longitudinal shear modulus of carbon fibre is calculated by [9]

$$G_{12} = \frac{\pi m L f^2 \left[8 \left(D_o^2 - D_i^2 \right) + \frac{32}{3} h^2 \right]}{d^4} \tag{1}$$

where m is the mass of the hanging washer; D_o and D_i are the outer and inner diameter of the washer, respectively; h is the thickness of the washer; d is the diameter of the fibre; L is the length of the fibre that has been suspended; f is the oscillation frequency; and G_{12} denotes the longitudinal shear modulus of fibre. The frequency was measured by a stopwatch with resolution of 0.01 s. The diameters of the fibres were measured by FE-SEM. The shear modulus tests were performed using four washers with different geometries at three fibre lengths: 15, 20 and 25 mm. Five samples were tested for each weight-length combination. The shear modulus values of different gauge lengths are consistent (see Table 3), suggesting the absence of significant damping factor in the case of long fibre and end effect in the case of short fibre length [9]. The shear modulus of the carbon fibre is determined to be 6.81±0.41 GPa, in good agreement with literature values for similar fibres [19, 20].

Because compressive strength and shear modulus of carbon fibre are both strongly affected by the cross-sectional microstructure and properties [35], a correlation between the two properties was established by Northolt et al. [36] as an approximate and linear function: $\sigma_C = -0.05(0.3) + 0.10(0.01)G$, (estimated standard deviation in parentheses). It implies that some factors may simultaneously influence the compressive strength and shear moduli. Such factors include lattice imperfection and covalent bonding between the basal planes [37, 38]. In the model, the fibre filament is considered as being built up of a parallel array of identical fibrils, which subject to a uniform stress along the filament axis. However, since the crystallites have an orientation distribution with respect to the filament axis, any form of disorder, usually occurring in polycrystalline carbons, decreases shear modulus [36]. On the other hand, high compressive strength correspond to high degree of order and the inherent structure. In addition, strong transverse forces, like covalent crosslinks, have a dual effect to increase the macroscopic shear modulus and improve the compressive properties [38]. Hence, an increase in shear modulus is usually accompanied by an increase in the compressive limit of the fibre. In this study, the correlation was verified by our result which fits well with the overall trend, as shown in Fig. 9.

Table 3 G_{12} of the carbon fibre obtained by torsional pendulum tests

No.	m (mg)	D_o (mm)	D_i (mm)	h (mm)	L (mm)	$\overline{f}$ (s^{-1})	$\overline{d}$ (μm)	$\overline{G}_{12}$ (GPa)	Mean of all tests (GPa)
1	725.1	12.8	6.6	1.0	15	0.0217	7.10	6.25	6.81±0.41
					20	0.0198	7.17	6.61	
					25	0.0182	7.23	6.79	
2	865.0	12.0	6.5	1.6	15	0.0247	7.23	7.61	
					20	0.0186	7.07	6.31	
					25	0.0184	7.18	7.27	
3	1183.6	16.8	8.6	1.0	15	0.0140	7.25	6.64	
					20	0.0123	7.30	6.59	
					25	0.0109	7.27	6.67	
4	1295.4	16.0	7.4	1.1	15	0.0136	7.17	6.84	
					20	0.0122	7.33	6.78	
					25	0.0109	7.20	7.35	

Transverse Modulus by Nano-indentation Test

Nano-indentation technique was employed to probe the transverse modulus (E_2) of the carbon fibre. The yarn, which consists of 12,000 fibres, was embedded in epoxy resin, and then polished to a flat surface parallel to the longitudinal direction of the fibres. Nano-indentation was made on the flat surface with the fibres revealed on the top surface. Such test on the impregnated yarn has two advantages. Firstly, fibres in the sample are restrained so that movements are prohibited, minimising the slippage interference. Secondly, different properties of carbon fibre and the epoxy matrix (and interphase) allow their distinctive load–displacement curves to be distinguished. Comparing the data obtained via nano-indentation with known epoxy properties will crosscheck the validity of carbon fibre properties measured by the same test.

The tests were performed on Agilent Nano Indenter G200 with a Berkovich tip. To provide a more precise measurement
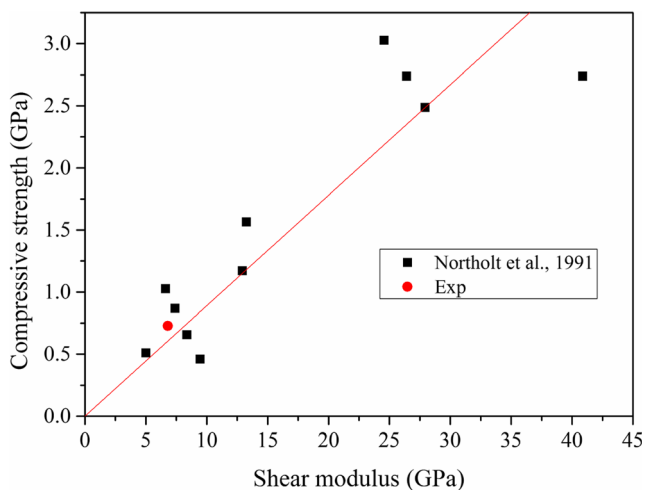
of initial surface contact, continuous stiffness measurement technique [39], as opposed to the conventional ones which utilise only the unloading path in the load–displacement curves, was employed in this study. Nano-indentations were performed along six indent lines, each consisting of 10 indent points with spacing of 20 μm, along the transverse direction at randomly chosen locations of the impregnated yarn. The tip indentation was controlled by a frequency of 45 Hz at the strain rate of 0.05 s^{-1}. The load was maintained for 30 s to evaluate the errors caused by temperature variations [16]. The Poisson's ratio of the carbon fibre was assumed to be ν=0.2 in the experiments.

Figure 10 shows the load-displacement curves and the relation between the measured modulus and displacement into surface (for clarity purpose, only representative curves are shown). Three different types of load-displacement can be identified, which represent the indentation response of the fibre, fibre-epoxy interphase region, and the epoxy. The curve

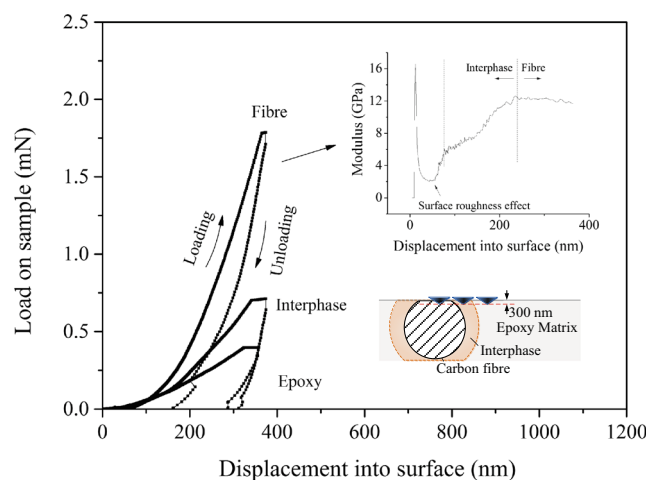**Fig. 9** Relationship between the compressive strength and the shear modulus of carbon fibres

Fig. 10 Load–displacement plot and relation between the displacement into surface and elastic modulus

that corresponds to epoxy is a hysteresis loop during the loading-unloading cycle while the curve of carbon fibre shows similar loading-unloading paths. The differences can be explained by the strain relaxation, viscoelasticity behaviour of epoxy matrix and the elastic behaviour of carbon fibre [40]. The curves with intermediate peak loads represent the interphase between fibre and matrix. In the interphase region, the mechanical properties of epoxy are different from the bulk. In addition, there is no single value of the modulus for the interphase region as the interphase closer to the carbon fibre is stiffer while the region closer to the epoxy is softer [41].

In the modulus–displacement plot (inset of Fig. 10), three segments can be identified as well. The first one is attributed
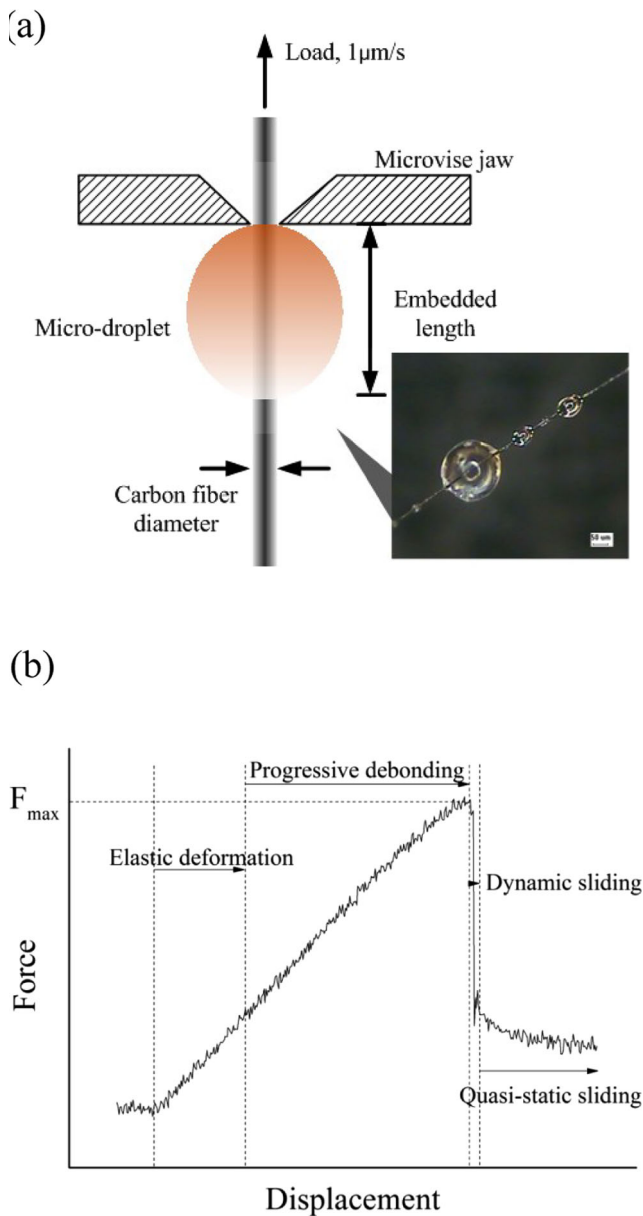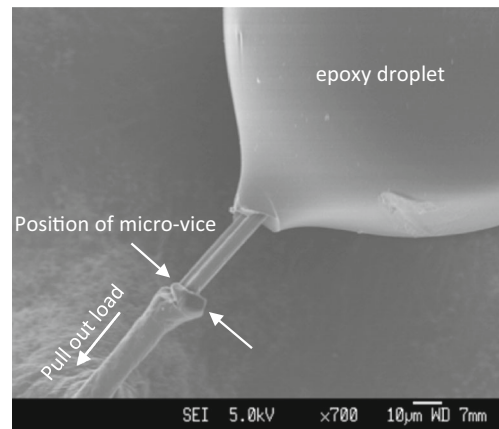

Fig. 12 Epoxy droplet pulled away from its original position (*arrow*)

to the heterogeneity and surface unevenness of the indentation sample which cannot be fully eradicated by polishing. The second one exhibits a hardening behaviour illustrating the nano-indenter's movement that approaches the carbon fibre by penetrating the interphase; and the third one, after around 230 nm, indicates the stabilisation of measured modulus. The maximum and minimum calculation depths were 330 and 280 nm, respectively, for estimating the elastic modulus. The E_2 of the carbon fibre was measured to be 13.4 ± 1.1 GPa, in line with values reported by others for similar fibres [11, 16, 39]. As an indirect verification, the Young's modulus of epoxy measured by our indentation test was 3.36 ± 0.35 GPa, matching very well the tensile-experiment-determined value of 3.4 GPa.

Interfacial Shear Strength Measurement by Microbond Test

The small diameter of carbon fibre and the large number of fibres in fibrous composites lead to a very high interfacial area
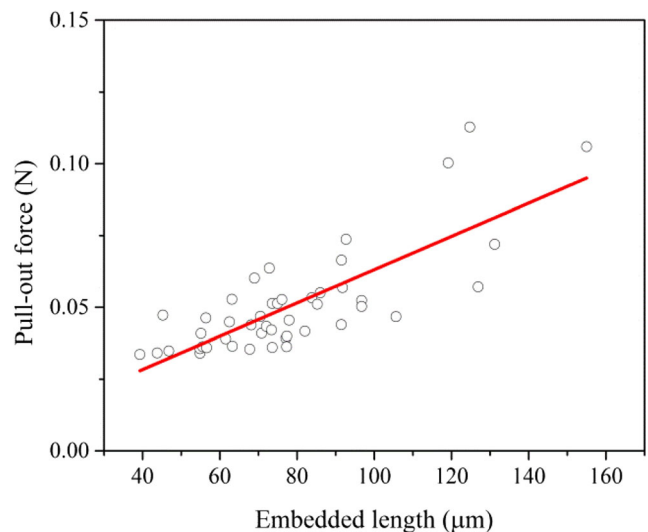

Fig. 11 (a) Microdroplet schematic and (b) representative load-displacement curve

Fig. 13 Relationship between fibre pull-out force and the fibre embedded length

per unit volume. As such, interface strength plays an important role in determining the mechanical properties of fibre-reinforced composites [12]. In this study, the apparent interfacial shear strength ($IFSS_{app}$) of carbon fibre/L20 epoxy interface was determined by the microbond test (see Fig. 11). Figure 11(b) shows a representative load-displacement curve and various stages during a microbond test.

The apparent $IFSS$ was defined as follows

$$IFSS_{app} = \frac{F}{\pi Dl} \tag{2}$$

where F is the peak pull-out force, D is fibre diameter and l is the embedded length of the fibre. Physically it refers to the average magnitude of shear stress at the point of interfacial failure.

In the experiment, an epoxy resin droplet was applied onto the fibre and cured for 24 h at room temperature followed by 15 h heat treatment at 60 °C. All the specimens were inspected under the microscope to examine the droplet shape and the embedded length. If the droplet is not axial-symmetric, it can be observed easily under microscope and the sample will be rejected. An integrated elliptical droplet was acceptable while any irregular and defective droplets were screened out before the test. Even if the defective droplet escaped the selection process and was tested in experiments, the debonding force would be significantly smaller than those from axial-symmetric droplets. These abnormal results were also rejected. The size requirement was that the droplets diameter should be smaller than 160 μm; otherwise the required pull-out force would exceed the breaking strength of the fibre (i.e., the fibres broke before pull-outs occurred). Figure 12 shows a pulled-out droplet and there is no residual epoxy on the fibre surface after debonding. It indicates that the adhesive failure did take place in the fibre/matrix interface.

$IFSS_{app}$ was calculated from the slope of regression line in the peak load- embedded length plot as shown in Fig. 13 to be 26.7 MPa. This value is in reasonable agreement with other documented values [42].

The properties measured in this paper are able to improve the accuracy of tensile strength predictions of braided textile composites fabricated using the carbon fibre. More research is currently being undertaken in our group, the results will be reported in the future.

Conclusions

Tests on a commercially obtained single carbon fibres were performed to determine their mechanical properties. The presence of defects, flaws and misoriented crystallites in the carbon fibre leads to the gauge-length-dependence phenomenon in the elastic modulus and strength along the longitudinal direction. Quasi-static tensile tests performed at different gauge lengths of 5, 10, 15, 20, 50, 100, 150 and 200 mm suggest that the tensile strength (σ_{t1}) of this carbon fibre decreases when gauge length increases, dropping from 3.8 to 2.1 GPa.

The longitudinal compressive strength (σ_{c1}) of the carbon fibre was determined by tensile recoil method to be 728.8 MPa. Longitudinal shear modulus (G_{12}) was obtained via the torsional pendulum test to be 6.81 GPa. The transverse Young's modulus (E_2) was measured with the aid of nano-indentation technique to be 13.4 GPa. To obtain the interfacial properties of the carbon fibre, microbond tests were carried out. The apparent interfacial shear strength ($IFSS_{app}$) of carbon fibre/L20 epoxy resin was 26.8 MPa. In summary, this study was able to provide results and ways to arrive at definite property values despite scatters for the carbon fibre. The applied test methodologies are useful for the characterization of other types of fibrous materials as well.

References

1. Edison TA (1882) Manufacture of Carbon Filaments. US Patent 411, 016
2. Ji XB, Khatri AM, Chia ESM et al (2013) Multi-scale simulation and FE-assisted computation of elastic properties of braided textile reinforced composites. J Compos Mater. doi:10.1177/0021998313480198
3. LLorca J, González C, Molina-Aldareguía JM, Segurado J et al (2011) Multiscale modeling of composite materials: a roadmap towards virtual testing. Adv Mater 23:5130–5147
4. Miravete A, Bielsa JM, Chiminelli A et al (2006) 3D mesomechanical analysis of three-axial braided composite materials. Compos Sci Technol 66:2954–2964
5. Ha SK, Jin KK, Huang Y (2008) Micro-Mechanics of Failure (MMF) for continuous fibre reinforced composites. J Compos Mater 42(18): 1873–1895
6. Li X, Binienda W, Goldberg R (2011) Finite-element model for failure study of two-dimensional triaxially braided composite. *J Aerospace Eng* 24, special issue: Mechanics of Advanced Materials and Structures: 170–180
7. Kumari S, Nithya S, Padmavathi N et al (2010) Tensile properties and fracture behaviour of carbon fibre filament materials. J Mater Sci 45: 192–200
8. Kumar S, Anderson DP, Crasto AS (1993) Carbon fibre compressive strength and its dependence on structure and morphology. J Mater Sci 28(2):423–439
9. Tsai CL, Daniel IM (1999) Determination of shear modulus of single fibres. Exp Mech 39:284–286
10. Lim J, Zheng JQ, Masters K, Chen WW (2010) Mechanical behavior of A265 single fibres. J Mater Sci 45:652–661
11. Miyagawa H, Mase T, Sato C et al (2006) Comparison of experimental and theoretical transverse elastic modulus of carbon fibres. Carbon 44:2002–2008
12. Rodríguez M, Molina-Aldareguía JM, González C, LLorca J (2012) A methodology to measure the interface shear strength by means of the fibre push-in test. Compos Sci Technol 72:1924–1932

13. Deteresa SJ, Farris RJ, Porter RS (1982) Behavior of an aramid fibre under uniform compression. Polym Compos 3(2):57–58

14. DeTeresa SJ, Allen SR, Farris RJ, Porter RS (1984) Compressive and torsional behaviour of Kevlar 49 fibre. J Mater Sci 19(1):52–72

15. DeTeresa SJ, Porter RS, Farris RJ (1985) A model for the compressive buckling of extended chain polymers. J Mater Sci 20(5):1645–1659

16. Maurin R, Davies P, Baral N, Baley C (2008) Transverse properties of carbon fibres by nano-indentation and micro-mechanics. Appl Compos Mater 15:61–73

17. Ueda M, Takiguchi T (1991) Measurement of transverse Young's modulus of fibres by angular characteristics of ultrasonic scattering. Adv Compos Mater 1(4):309–320

18. Sun XS, Tan VBC, Tay TE (2011) Micromechanics-based progressive failure analysis of fibre-reinforced composites with non-iterative element-failure method. Comput Struct 89(11–12):1103–1116

19. Li X (2010) Mesomechanical model for failure study of two dimensional triaxial braided composite materials, PhD Dissertation, The University of Akron

20. Bacarreza O, Aliabadi MH, Apicella A (2012) Multi-scale failure analysis of plain-woven composites. J Strain Anal Eng 47(6):379–388

21. Gibson RF (1994) Principles of composite materials mechanics. McGraw-Hill, New York

22. Swift C (2012) Specialty Fibers: Technologies and Global Markets. Market Research Report, BCC Research

23. Weibull W (1939) A statistical theory of the strength of materials. Ing Vetenskaps Akad Handl 151:5

24. van der Zwaag S (1989) The concept of filament strength and the Weibull modulus. J Test Eval 17(5):292–298

25. Waterbury MC, Drzal LT (1991) On the determination of fiber strengths by in-situ fiber strength testing. Compos Sci Technol Res 13:22–28

26. Reynolds WN, Sharp JV (1974) Crystal shear limit to carbon fibre strength. Carbon 12:103–110

27. Zohdi TI, Powell D (2006) Multiscale construction and large-scale simulation of structural fabric undergoing ballistic impact. Comput Method Appl Mech 195:94–109

28. Macturk KS, Eby RK, Adams WW (1991) Characterization of compressive properties of high-performance polymer fibres with a new microcompression apparatus. Polymer 32(10):1782–1787

29. Sinclair D (1950) A bending method for measurement of the tensile strength and Young's modulus of glass fibres. J Appl Phys 21:380–386

30. Hawthorne HW, Teghtsoonian E (1975) Axial compression fracture in carbon fibres. J Mater Sci 10(1):41–51

31. Oya N, Johnson DJ (2001) Longitudinal compressive behaviour and microstructure of PAN-based carbon fibres. Carbon 39(5):635–645

32. Allen SR (1987) Tensile recoil measurement of compressive strength for polymeric high performance fibres. J Mater Sci 22:853–859

33. Kumar IP, Mohite PM, Kamle S (2013) Axial compressive strength testing of single carbon fibres. Arch Mech 65(1):27–43

34. Jiang H, Abhiraman AS, Tsui K (1993) Analysis of failure in 'recoil from tension' of pan-based carbon fibres. Carbon 31(6):887–894

35. Chung DDL (1994) Carbon fibre composites. Butterworth-Heinemann, Boston

36. Northolt MG, Veldhuizen LH, Jansen H (1991) Tensile deformation of carbon fibres and the relationship with the modulus for shear between the basal planes. Carbon 29(8):1267–1279

37. Dobb MG, Johnson DJ, Park CR (1990) Compressional behavior of Carbon Fibers. J Mater Sci 25(2):829–834

38. Oya N, Johnson DJ (1999) Direct measurement of longitudinal compressive strength in carbon fibres. Carbon 37(10):1539–1544

39. Agilent Technologies (2013) Agilent Nano Indenter G200, http://cp.literature.agilent.com/litweb/pdf/5990-4172EN.pdf. Accessed 22 Jan 2014

40. Molazemhosseini A, Tourani H, Naimi-Jamal MR, Khavandi A (2013) Nanoindentation and nanoscratching responses of PEEK based hybrid composites reinforced with short carbon fibres and nano-silica. Polym Test 32:525–534

41. Tsujikami T, Horikawa T, Hirosawa S, Zako M (2006) Approach to analysis of mechanical behavior of textile composites by inclusion element method. JSME Int J A Mech M 49(3):418–425

42. Choi NS, Park JE, Kang SK (2009) Quasi-disk type microbond pull-out test for evaluating fibre/matrix adhesion in composites. J Compos Mater 43:1663–1677